

Electronic Supplementary Information

Dicyclopentadithienothiophene (DCDTT)-based Organic Semiconductor Assisted Grain Boundary Passivation for Highly Efficient and Stable Perovskite Solar Cells

Shakil N. Afraj,^a Arulmozhi Velusamy,^a Chung-Yu Chen,^a Jen-Shyang Ni,^b Yamuna Ezhumalai,^{a,c} Chun-Huang Pan,^a Kuan-Yu Chen,^d Shueh-Lin Yau,^a Cheng-Liang Liu,^e Chien-Hung Chiang,^{a,d*} Chun-Guey Wu,^{a,d*} Ming-Chou Chen^{a*}

^aDepartment of Chemistry, National Central University, Taoyuan 32001, Taiwan.

^bDepartment of Chemical and Materials Engineering, Photo-sensitive Material Advanced Research and Technology Center (Photo-SMART), National Kaohsiung University of Science and Technology, Kaohsiung 80778, Taiwan.

^cCentre for Material Chemistry, Karpagam Academy of Higher Education, Coimbatore-641021, India.

^dResearch center of new generation light driven photovoltaic modules, National Central University, Taoyuan 32001, Taiwan.

^eDepartment of Materials Science and Engineering, National Taiwan University, Taipei, 10617 Taiwan.

Corresponding Authors:

*Chien-Hung Chiang (E-mail: chiang95@cc.ncu.edu.tw)

*Chun-Guey Wu (E-mail: t610002@ncu.edu.tw)

*Ming-Chou Chen (E-mail: mcchen@ncu.edu.tw)

Table of Contents

Experimental Section

Characterization

Synthetic procedure for final compounds 1-3

Scheme S1. Synthesis of compound **6**

Scheme S2. Synthesis of **DCDTT (9)**

Scheme S3. Synthesis of compound **10**

Scheme S4. Synthesis of compound **13**

Figure S1. Reported molecular structures of (a) NFAs for grain boundary passivation of PSCs; (b) Donor passivating agents for PSCs; (c) A-D-A type small molecules for PSCs.

Figure S2. TGA curves of the studied compounds **1-3**.

Figure S3. DPV curves of the studied compounds **1-3**.

Figure S4. The UPS of the perovskite made by using pure CB (pristine perovskite), 0.2 wt% **IN-DCDTT (1)**, 0.2 wt% **IN^{Cl}-DCDTT (2)** or 0.2 wt% **IN^{Br}-DCDTT (3)** in CB as an anti-solvent (0.2 wt% compounds **1-3** treated perovskite).

Figure S5. The tauc plot of the pristine perovskite and perovskite films treated with 0.2 wt% compounds **1-3**.

Table S1. The energy level of pristine perovskite and perovskite films treated with 0.2 wt% compounds **1-3**.

Figure S6. UV-Vis absorption spectra of pristine perovskite and perovskite films treated with 0.2 wt% compounds **1-3**.

Figure S7a-c. FTIR spectrum of compounds **1-3** and compounds **1-3** mixed with PbI_2 .

Table S2. PL spectra of perovskite films on glass and FTO/ TiO_2 substrates.

Table S3. TRPL spectra of perovskite films with **Spiro-OMeTAD** overlayer.

Figure S8. (a) Device architecture of PSCs and (b) Schematic of grain boundary passivation by **IN^{Cl}-DCDTT (2)**.

Table S4. The I-V curves of the cell based on **IN^{Cl}-DCDTT (2)** treated perovskite measured with two voltage scan directions.

Table S5. The I-V curves of the cell based on pristine perovskite measured with two voltage scan directions.

Table S6. The integrated photocurrent density from IPCE and short-circuit current density from J-V of the reference cell and cells based on compounds **1-3**-treated perovskite films

Figures S9. The efficiency distribution for perovskite solar cells based on **IN^{Cl}-DCDTT (2)** treated perovskite absorbers (30 devices, average PCE of 20.15 ± 0.46)

Figure S10. The I-V curves of the perovskite films made by using CB, 0.2 wt% **IN-DCDTT (1)_(CB)**, 0.2 wt% **IN^{Cl}-DCDTT (2)_(CB)** or 0.2 wt% **IN^{Br}-DCDTT (3)_(CB)** as an anti-solvent.

Table S7. The conductivity of the perovskite film made by using CB, 0.2 wt% **IN-DCDTT (1)_(CB)**, 0.2 wt% **IN^{Cl}-DCDTT (2)_(CB)** or 0.2 wt% **IN^{Br}-DCDTT (3)_(CB)** as an anti-solvent.

¹H NMR spectra of synthesized compounds.

¹³C NMR spectra of synthesized compounds.

HRMS spectra of synthesized compounds.

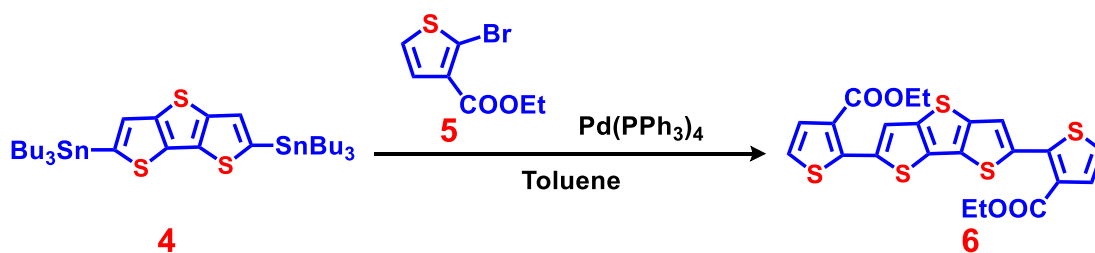
References

Experimental Section

Characterization

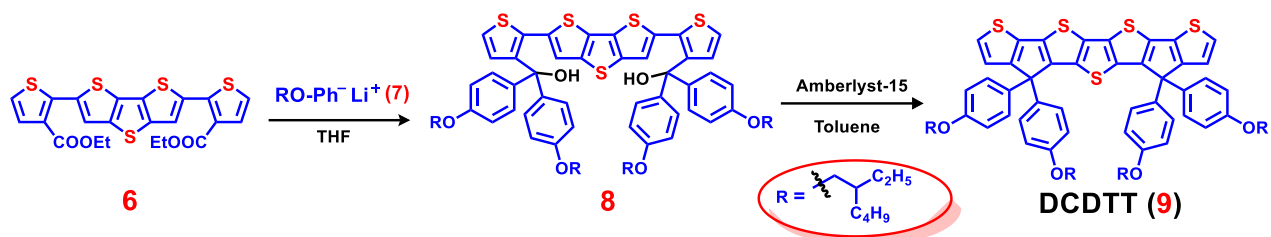
^1H and ^{13}C NMR spectra were recorded using a Bruker 500 or a 300 instrument, with reference to solvent signals. Differential scanning calorimetry (DSC) was carried out on a Mettler DSC 822 instrument at a scan rate of 10 K/min. Thermo gravimetric analysis (TGA) was performed on a Perkin Elmer TGA-7 thermal analysis system using dry nitrogen as a carrier gas at a flow rate of 40 mL/min. UV–Vis absorption and fluorescence spectra were obtained in the indicated solvents at room temperature using JASCO V-530 and Hitachi F-4500 spectrometers, respectively. Differential pulse voltammetry experiments were performed with a conventional three-electrode configuration (a platinum disk working electrode, an auxiliary platinum wire electrode, and a non-aqueous Ag reference electrode, with a supporting electrolyte of 0.1 M tetrabutylammonium hexafluorophosphate (dry TBAPF₆) in the specified dry solvent, using a CHI621C Electrochemical Analyzer (CH Instruments). Under N₂, the anhydrous OSC material was dissolved in above 0.1 M *o*-C₆H₄Cl₂ solution to prepare a 10⁻³ M test solution. In each DPV experiment, 5 mL of the test solution is scanned together with Fc⁺/Fc (also 10⁻³ M; as internal standard) under N₂. Electrochemical potentials were referenced to an Fc⁺/Fc internal standard (at +0.64 V). Mass spectrometric data were obtained with a JMS-700 HRMS instrument. Grazing incidence XRD data were collected in the 2θ range of 5–50 degree on a Bruker powder diffractometer (D8 Discover) using Cu Kα₁ radiation equipped with a 2D detector. UPS and X-ray photoelectron spectroscopy spectra were obtained from a Thermo VG-Scientific/VG-Sigma Probe spectrometer. UV/Vis and PL spectra were recorded using a Cary 300 Bio spectrometer and a Hitachi F-7000 fluorescence spectrophotometer, respectively, at room temperature. The nanosecond TRPL spectra were recorded with an opticalmicroscope-based system (UniRAM, Protrustech with the custom designed light path). The average power, wavelength, pulse duration, and repetition rate of the excitation are 20 μW, 405 nm, 150 ps, and 20 MHz, respectively. SEM was performed with a Hitachi S-800 microscope at 15 KV. Samples for SEM imaging were mounted on a metal stub with a piece of conducting tape and then coated with a thin layer of gold film to avoid charging. The cross-sectional SEM image was used for estimating

the film thickness and observing the interface contact between each layer of the cell. The contact angle was measured with a home-made set-up (Grandhand Ctag01, Taiwan) using water as a probe solvent. The contact angle is determined using the image of a sessile drop at the points of the intersection between the drop contour and the projection of the surface. Fourier transform infrared (FTIR) spectra were recorded for **IN^X-DCDTT** derivatives and **IN^X-DCDTT** derivatives+PbI₂ film in KBr using a Bio-Rad 155 FTIR spectrometer at ambient temperature with a resolution of 4 cm⁻¹. The electron-only devices were fabricated with the architecture FTO/c-TiO₂/m-TiO₂/various perovskite/ phenyl-C₆₁-butyric acid methyl ester (PCBM)/Ag, and measurement the dark I-V characteristics were evaluated to trap state density and charge mobility in the vertical direction of the various films.¹



Scheme S1. Synthesis of Compound 6

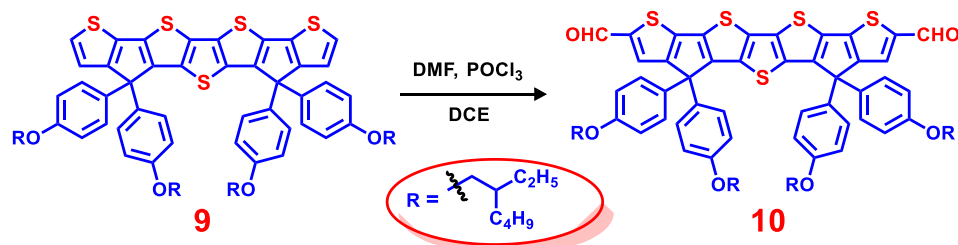
Synthesis of diethyl 2,2'-(dithieno[3,2-b:2',3'-d]thiophene-2,6-diyl)bis(thiophene-3-carboxylate) (6): Under anhydrous and deoxygenated conditions Pd(PPh₃)₄ (150 mg, 0.13 mmol) was added to the solution of bis(tributylstannyl)dithieno[3,2-b:2',3'-d]thiophene (**4**) (2.0 g, 2.7 mmol), ethyl 2-bromothiophene-3-carboxylate (**5**) (1.88 g, 8.1 mmol) and toluene (20 ml). The resulting mixture was refluxed for two days under nitrogen. After cooling to room temperature, the solvent was evaporated, the crude material was purified by column chromatography (15% EA/Hexane) to give product **6** as yellow solid, (1.0 g, 80%). ¹H NMR (300 MHz, CDCl₃) : δ (ppm) 7.74 (s, 2H), 7.52 (d, *J* = 5.4 Hz, 2H), 7.23 (d, *J* = 5.4 Hz, 2H), 4.32 (q, *J* = 7.2 Hz, 4H), 1.33 (t, *J* = 7.2 Hz, 6H); ¹³C NMR (125 MHz, CDCl₃): δ 163.06, 142.96, 141.58, 135.00, 132.32, 130.75, 128.22, 124.24, 122.60, 60.90, 14.25. HRMS (MALDI, [M]⁺) calcd for C₂₂H₁₆O₄S₅, 503.9652; Found: 503.9647.



Scheme S2. Synthesis of **DCDTT (9)**

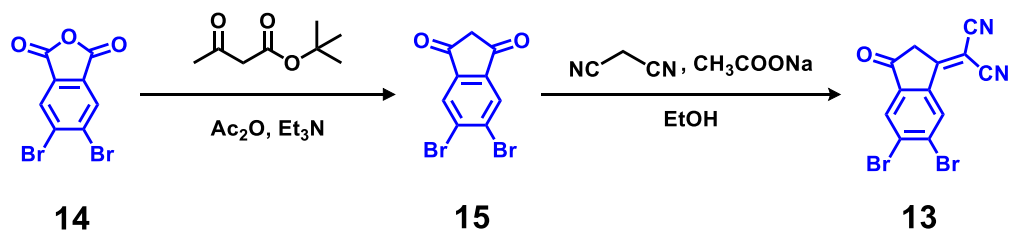
Synthesis of DCDTT (9): 2.5 M *n*-BuLi (3.3 mL in Hexanes, 8.3 mmol) was slowly added to 1-bromo-4-((2-ethylhexyl)oxy)benzene (2.28 g, 8 mmol) at -78 °C in THF (30 ml) under anhydrous condition, the mixture was stirred for one hour and then it was warmed to 0 °C to remove the formed C₄H₉Br in the reaction by vacuum, then THF (30 mL) was added and transferred anion (7) slowly to reaction flask containing to solution of diethyl 2,2'-(dithieno[3,2-b:2',3'-d]thiophene-2,6-diyl)bis(thiophene-3-carboxylate (**6**) (0.5 g, 1 mmol) (70 mL) in THF (70 mL) under anhydrous condition at -78 °C. Further, reaction mixture was slowly warmed to room temperature and heated to reflux for 2 hours. Further, reaction mixture was slowly warmed to room temperature and reaction was quenched by slow addition of deionized water and, THF was removed by rotary evaporator and reaction mixture was extracted by ether. Organic layer was dried over MgSO₄ and concentrated to give crude reaction mixture of benzylic alcohol **8** which was confirmed by ¹H NMR ((¹H NMR (500 MHz, CDCl₃): δ (ppm) 7.15-7.13 (m,10H), 6.83-6.81 (m,10H), 6.50 (d, *J* = 5.5 Hz, 2H), 3.83 (d, *J* = 5.5 Hz, 8H), 3.23 (s, 2H), 1.70 (m, 4H), 1.40 (m, 16H), 1.30 (m, 16H), 0.8 (m, 24H)) (Note. benzylic alcohol **8** is not enough stable to collect useful ¹³C NMR spectrum) and used for next step without further purification. To this crude reaction mixture toluene 30 ml followed by Amberlyst-15 was (0.5 g) was added under N₂ atmosphere and reaction mixture was refluxed for 4 hours. Further, reaction mixture was cool down to room temperature. toluene was removed under rotary evaporator and extracted with ethyl acetate and organic layer was dried over MgSO₄ and concentrated to give crude reaction mixture which is purified by column chromatography using DCM/Hexane (20:80) to give orange liquid (0.5 g, 41%). ¹H NMR (500 MHz, CDCl₃) : δ (ppm) 7.19 (d, *J* = 5 Hz, 2H), 7.12 (d, *J* = 8.5 Hz, 8H), 7.01 (d, *J* = 5 Hz, 2H), 6.74 (d, *J* = 9 Hz, 8H), 3.76 (m,

8H), 1.70 (m, 4H), 1.40 (m, 32H), 0.8 (m, 24H). ^{13}C NMR (125 MHz, CDCl_3): δ 158.49, 157.93, 149.27, 136.40, 136.21, 135.37, 134.10, 132.18, 128.87, 125.72, 123.13, 114.44, 70.31, 61.46, 39.44, 30.54, 29.12, 23.86, 23.06, 14.10, 11.15. HRMS (MALDI, $[\text{M}]^+$) calcd for $\text{C}_{74}\text{H}_{88}\text{O}_4\text{S}_5$, 1200.5286; Found: 1200.5281.



Scheme S3. Synthesis of compound **10**.

Synthesis of compound 10: Slowly POCl_3 (3 mL) was added to DMF (2 mL) in 30 mL DCE at 0°C and stirred for 30 min at same temperature. To this solution, **DCDTT (9)** (0.5 g, 0.19 mmol) was added 0°C and refluxed for 20 hours. Reaction mixture was cooled to room temperature and slowly saturated solution of NaHCO_3 was added at 0°C and warmed to RT. Reaction mixture was extracted with ethyl acetate, organic layer was concentrated and crude residue was purified by column chromatography (EA/Hexane 15:85) to obtain compound **10** as orange liquid (0.3 g 57%). ^1H NMR (300 MHz, CDCl_3) : δ (ppm) 9.80 (s, 2H), 7.62 (s, 2H), 7.10 (d, $J = 8.7$ Hz, 8H), 6.77 (d, $J = 8.7$ Hz, 8H), 3.76 (m, 8H), 1.68 (m, 4H), 1.44 (m, 16H), 1.41 (m, 16H), 0.90 (m, 24H). ^{13}C NMR (125 MHz, CDCl_3): δ 182.30, 158.90, 158.45, 153.20, 146.49, 144.28, 136.79, 136.29, 136.12, 135.24, 132.56, 131.27, 128.67, 114.71, 70.42, 61.79, 39.39, 31.92, 30.50, 30.48, 30.33, 29.69, 29.65, 29.35, 29.07, 23.82, 23.01, 22.68, 14.09, 14.04, 11.10, 11.07. HRMS (MALDI, $[\text{M}]^+$) calcd for $\text{C}_{76}\text{H}_{88}\text{O}_6\text{S}_5$, 1256.5184 Found : 1256.5181.



Scheme S4. Synthesis of compound **13**.

Synthesis of 5,6-dibromo-1H-indene-1,3(2H)-dione (15): To the mixture of 4,5-dibromophthalic anhydride (1 g, 3.27 mmol), acetic anhydride (4 mL) and, triethylamine (2 mL) in volume ratio 2:1 was slowly added tertbutylacetoacetate (0.517 g, 6.32 mmol) and reaction mixture was stirred overnight. Further, reaction was quenched with ice and concentrated hydrochloric acid, then heated at 80°C for 1 hour. The reaction mixture was cooled to room temperature and preprecipitated solid was obtained by vacuum filtration, (0.89 g, 89%). ¹H NMR (300 MHz, CDCl₃) : δ (ppm) 8.22 (s, 2H), 3.25 (s, 2H).

2-(5,6-dibromo-3-oxo-2,3-dihydro-1H-inden-1-ylidene)malononitrile (13): Mixture of 5,6-dibromo-1,3-indandione (1 g, 3.29 mmol) and malononitrile (0.434 mg, 6.58 mmol) sodium acetate (0.405 g, 4.94 mmol), in ethanol (20 mL) was stirred at room temperature for 1 hour, and then heated for 3 hour. Further, reaction mixture added to water and ethanol mixture (20 mL) acidified with an aqueous hydrochloric acid, and precipitated solid was filtered by vacuum filtration and washed with hexane to get compound **13** (0.903 g, 78%). ¹H NMR (300 MHz, CDCl₃) : δ (ppm) 8.90 (s, 1H), 8.22 (s, 1H), 3.76 (s, 2H).

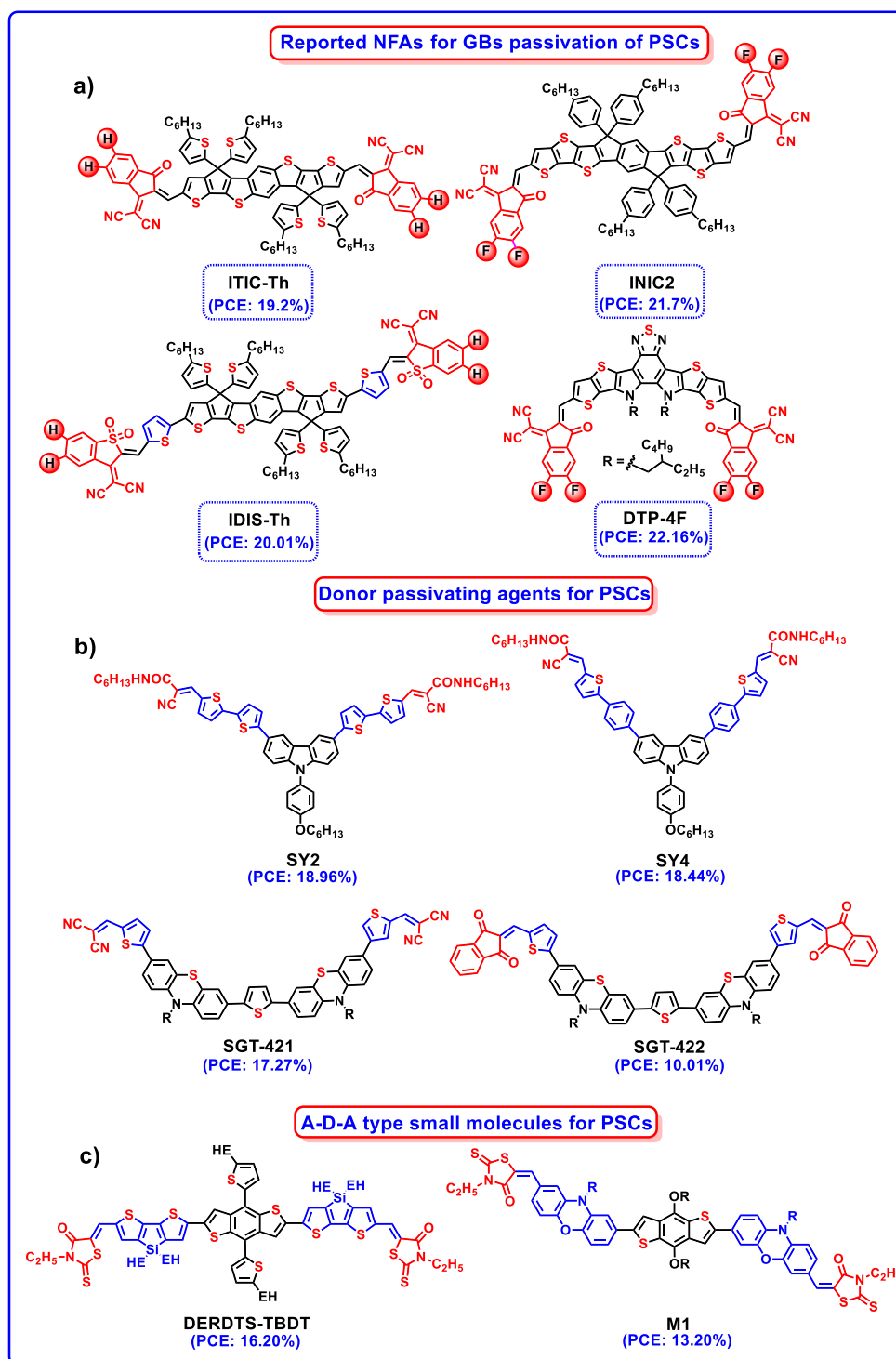


Figure S1. Reported molecular structures of (a) NFAs for grain boundary passivation of PSCs; (b) Donor passivating agents for PSCs; (c) A-D-A type small molecules for PSCs.

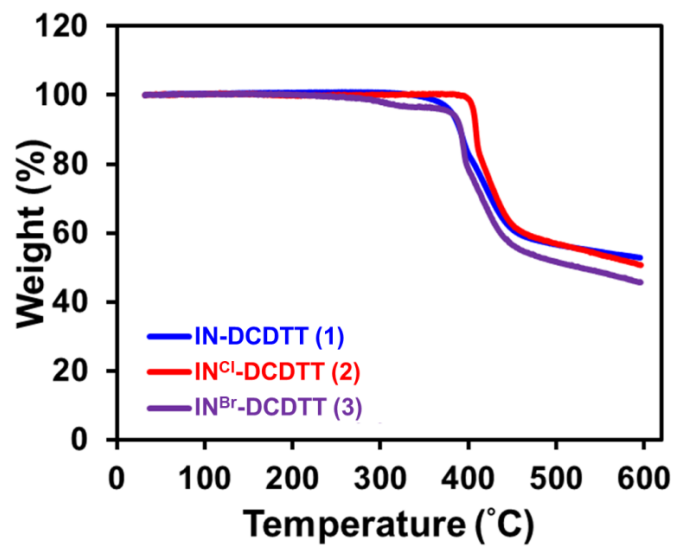


Figure S2. TGA curves of the studied compounds 1-3.

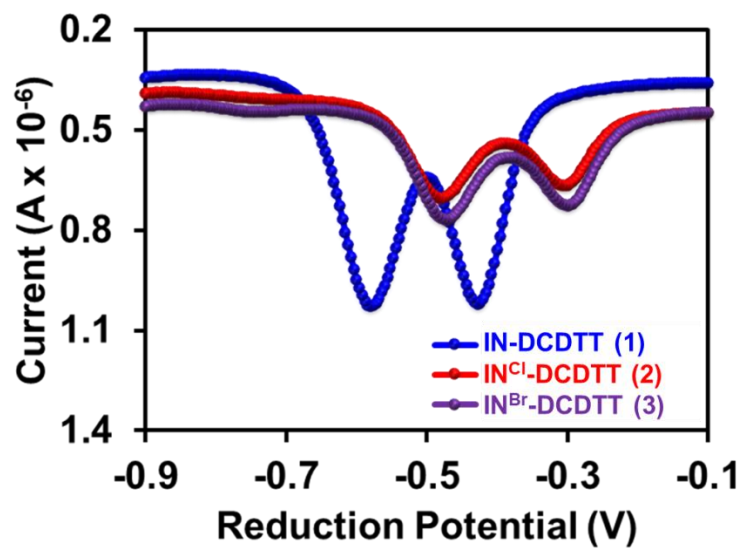


Figure S3. DPV curves of the studied compounds 1-3.

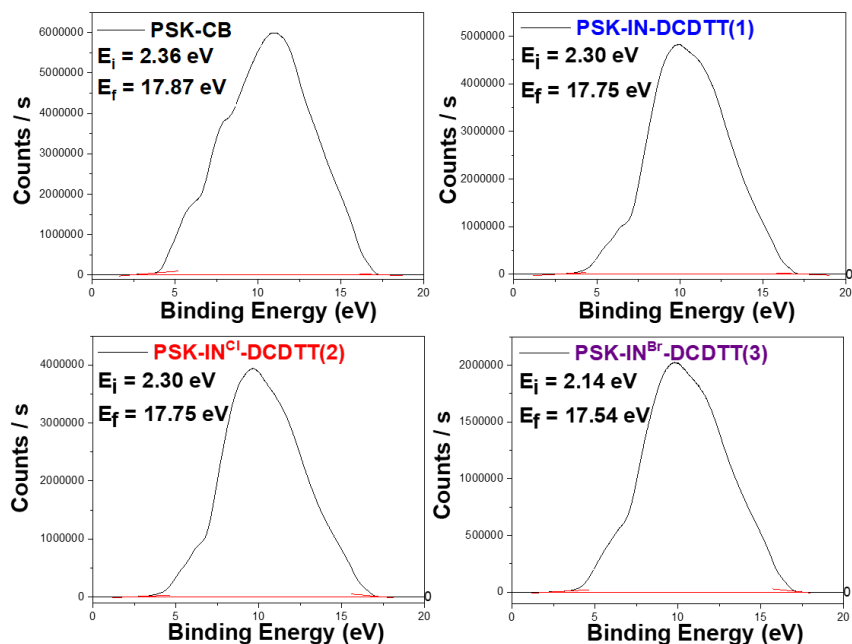


Figure S4. The UPS of the perovskite made by using pure CB (pristine perovskite), 0.2 wt% IN-DCDTT (1), 0.2 wt% IN^{Cl}-DCDTT (2) or 0.2 wt% IN^{Br}-DCDTT (3) in CB as an anti-solvent (0.2 wt% compounds 1-3 treated perovskite).

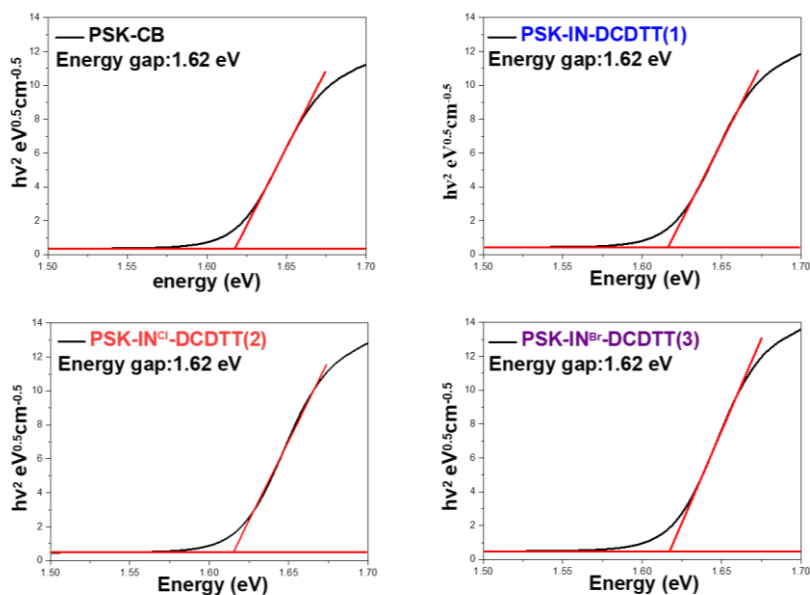


Figure S5. The tauc plot of the pristine perovskite and perovskite films treated with 0.2 wt% compounds **1-3**.

Table S1. The energy level of pristine perovskite and perovskite films treated with 0.2 wt% compounds **1-3**.

Film	CB (eV)	E _g (eV)	VB (eV)
PSK-CB	-5.69	1.62	4.07
PSK-IN-DCDTT-(1)	-5.75	1.62	4.13
PSK-IN ^{Cl} -DCDTT-(2)	-5.81	1.62	4.19
PSK-IN ^{Br} -DCDTT-(3)	-5.80	1.62	4.18

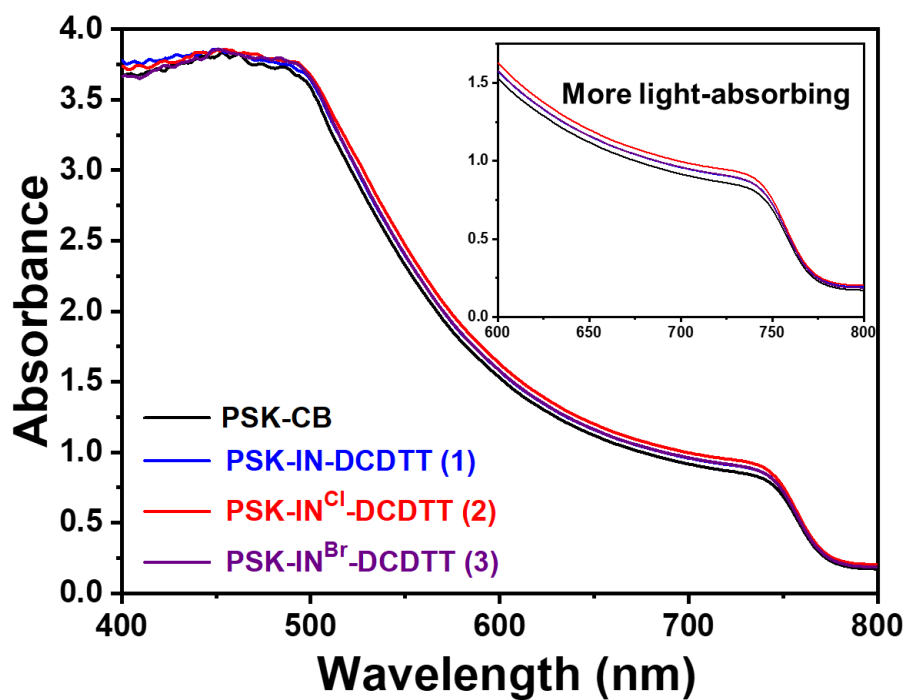


Figure S6. UV-Vis absorption spectra of pristine perovskite and perovskite films treated with 0.2 wt% compounds **1-3**.

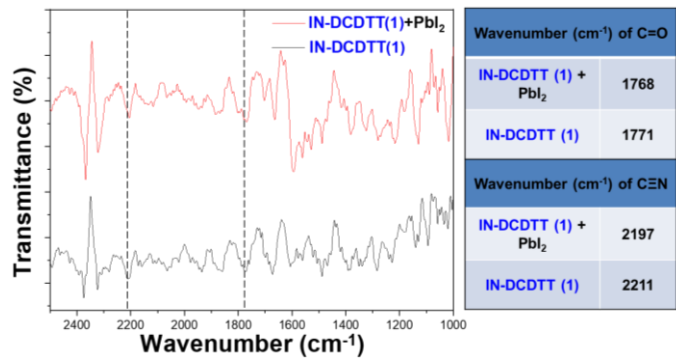


Figure S7a. FTIR spectrum of IN-DCDTT (1) and IN-DCDTT (1) mixed with PbI₂.

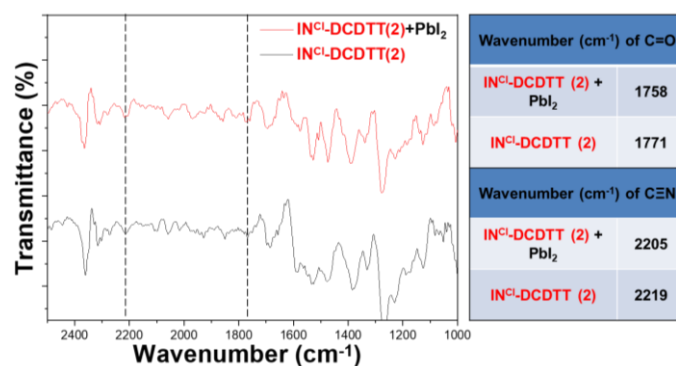


Figure S7b. FTIR spectrum of IN^{Cl}-DCDTT (2) and IN^{Cl}-DCDTT (2) mixed with PbI₂.

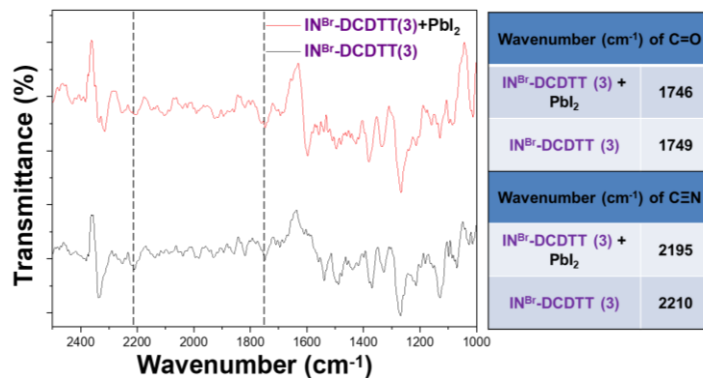


Figure S7c. FTIR spectrum of IN^{Br}-DCDTT (3) and IN^{Br}-DCDTT (3) mixed with PbI₂.

Table S2. PL spectra of perovskite films on glass and FTO/TiO₂ substrates.

Sample	PL intensity	^a Charge injection/transfer efficiency (η_{inj})
CB on glass	70	--
0.2 wt% IN-DCDTT _(CB) on glass	145	--
0.2 wt% IN ^{Cl} -DCDTT _(CB) on glass	242	--
0.2 wt% IN ^{Br} -DCDTT _(CB) on glass	198	--
CB onTiO ₂	47	33%
0.2 wt% IN-DCDTT _(CB) onTiO ₂	35	76%
0.2 wt% IN ^{Cl} -DCDTT _(CB) onTiO ₂	3	99%
0.2 wt% IN ^{Br} -DCDTT _(CB) onTiO ₂	27	86%

^a Charge injection efficiency (η_{inj}) = (Δ PL)/PL

Table S3. TRPL spectra of perovskite films with Spiro-OMeTAD overlayer.

Films	A1	τ_1 lifetime (ns)	A2	τ_2 lifetime (ns)	τ_{av} (ns)
PSK-CB with Spiro-OMeTAD	0.65	0.94	0.35	3.19	1.73
PSK- IN-DCDTT (1) with Spiro-OMeTAD	0.69	0.62	0.31	2.68	1.26
PSK- IN ^{Cl} -DCDTT (2) with Spiro-OMeTAD	0.78	0.22	0.22	1.21	0.44
PSK- IN ^{Br} -DCDTT (3) with Spiro-OMeTAD	0.73	0.31	0.27	2.23	0.83

$$y = A_1 * \exp(-t/T_1) + A_2 * \exp(-t/T_2)$$

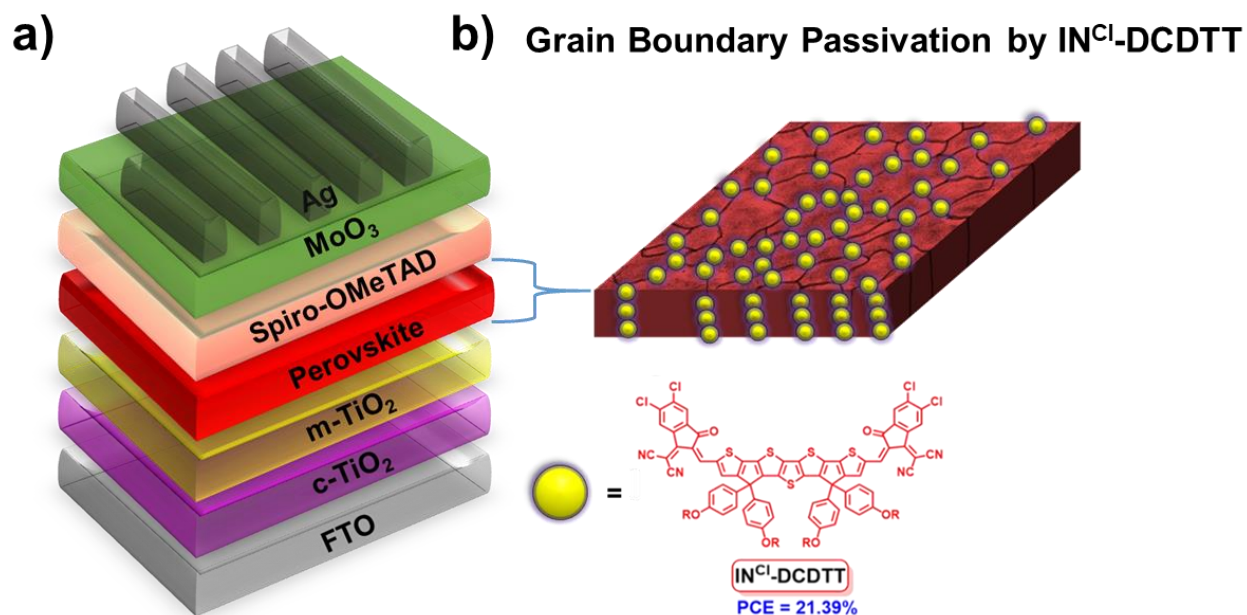


Figure S8. (a) Device architecture of PSCs and (b) Schematic of grain boundary passivation by IN^{Cl}-DCDTT (2).

Table S4. The I-V curves of the cell based on IN^{Cl}-DCDTT (2) treated perovskite measured with two voltage scan directions.

$$\text{Hysteresis index} = (\text{PCE}_{\text{reverse}} - \text{PCE}_{\text{forward}}) / \text{PCE}_{\text{reverse}}$$

Direction	Jsc (mA/cm ²)	Voc (V)	FF	FF%	Hysteresis Index
Negative to positive bias	23.71	1.10	0.82	21.39	0.5%
Positive to negative bias	23.67	1.11	0.81	21.28	

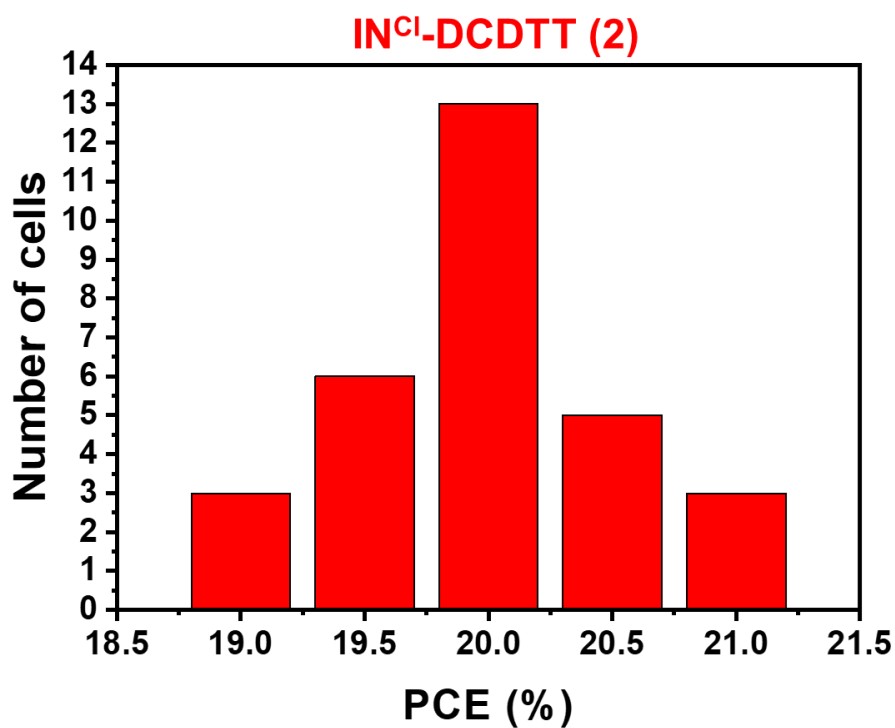
Table S5. The I-V curves of the cell based on pristine perovskite measured with two voltage scan directions.

Direction	Jsc (mA/cm ²)	Voc (V)	FF	FF%	Hysteresis Index
Negative to positive bias	21.98	0.73	17.00	17	18.94%
Positive to negative bias	21.36	0.68	13.72	13.72	

$$\text{Hysteresis index} = (\text{PCE}_{\text{reverse}} - \text{PCE}_{\text{forward}}) / \text{PCE}_{\text{reverse}}$$

Table S6. The integrated photocurrent density from IPCE and short-circuit current density from J-V of the reference cell and cells based on compounds **1-3**-treated perovskite films

Anti-solvent	Integrated Photocurrent Density from IPCE (mA/cm ²)	Short-circuit Current from J-V
CB	19.75	21.98
0.2wt% IN-DCDTT (1)	20.98	22.52
0.2wt% IN ^{Cl} -DCDTT (2)	22.22	23.71
0.2wt% IN ^{Br} -DCDTT (3)	21.77	23.32



Figures S9. The efficiency distribution for perovskite solar cells based on IN^{Cl}-DCDTT (2) treated perovskite absorbers (30 devices, average PCE of 20.15 ± 0.46)

The trap density was determined using the following equation:

$$n_{trap} = \frac{2\varepsilon_0\varepsilon_r V_{TFL}}{eL^2}$$

Where ε_0 is the vacuum permittivity, ε_r is the relative dielectric constant, V_{TFL} is the onset voltage of the trap-filled limit region, e is the elementary charge, and L is the distance between the electrodes. The electron mobility was further extracted using Mott-Gurney Law.²

Film	n_{trap}
PSK-CB	$1.61 \times 10^{16} \text{ cm}^{-3}$
PSK-IN ^{Cl} -DCDTT (2)	$7.14 \times 10^{15} \text{ cm}^{-3}$

The electron mobility

The electron mobility can be by the following version of the Mott–Gurney equation:

$$J = \frac{9\varepsilon\varepsilon_0\mu V^2}{8L^3}$$

Here, ε_0 is the permittivity of free space, ε is the dielectric constant of the material, L is the thickness of the perovskite film, and V is the applied voltage.³

Film	Mobility
PSK-CB	3.50×10^{-4}
PSK-IN ^{Cl} -DCDTT (2)	7.47×10^{-3}

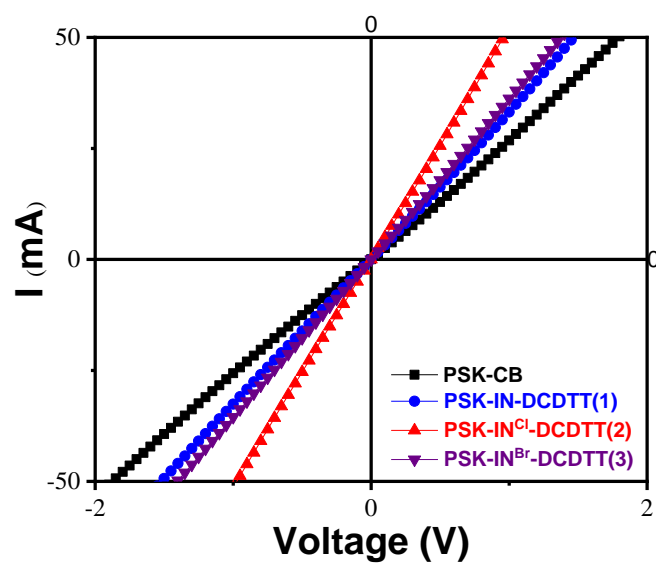


Figure S10. The I-V curves of the perovskite films made by using CB, 0.2 wt% **IN-DCDTT (1)_(CB)**, 0.2 wt% **IN^{Cl}-DCDTT (2)_(CB)** or 0.2 wt% **IN^{Br}-DCDTT (3)_(CB)** as an anti-solvent.

$$\sigma_0 = Id / AV$$

σ_0 : Conductivity

I: Current

A: Detected area (0.1 cm²)

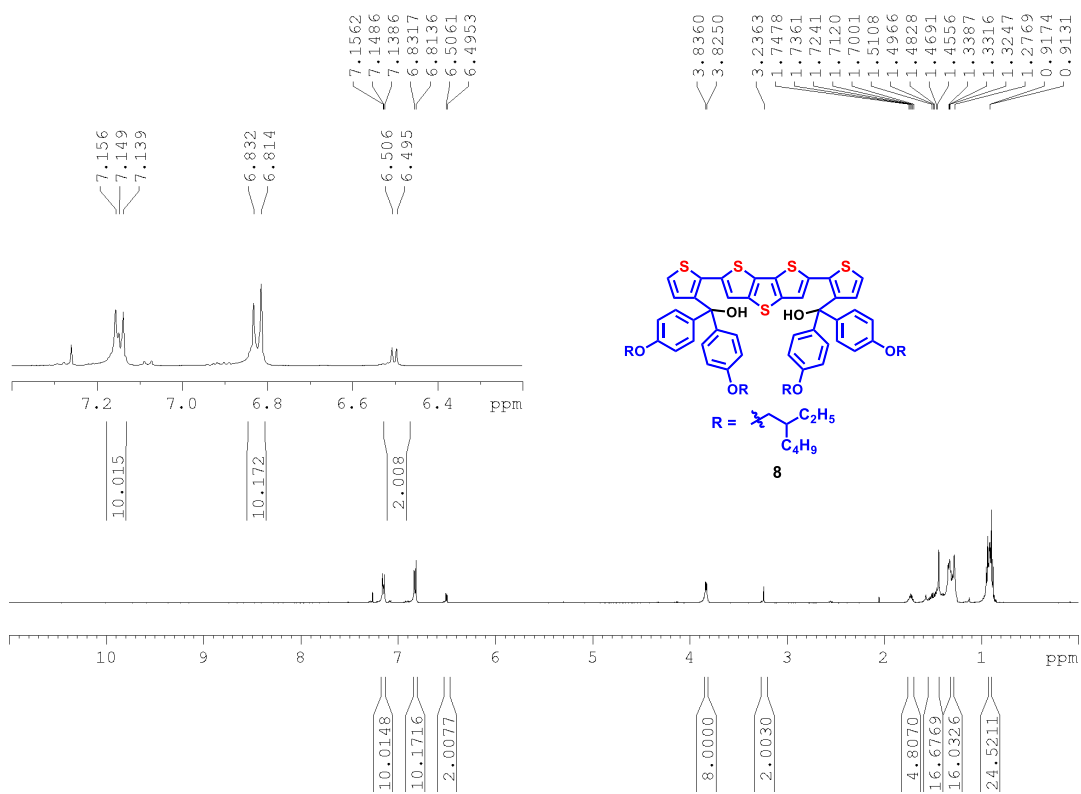
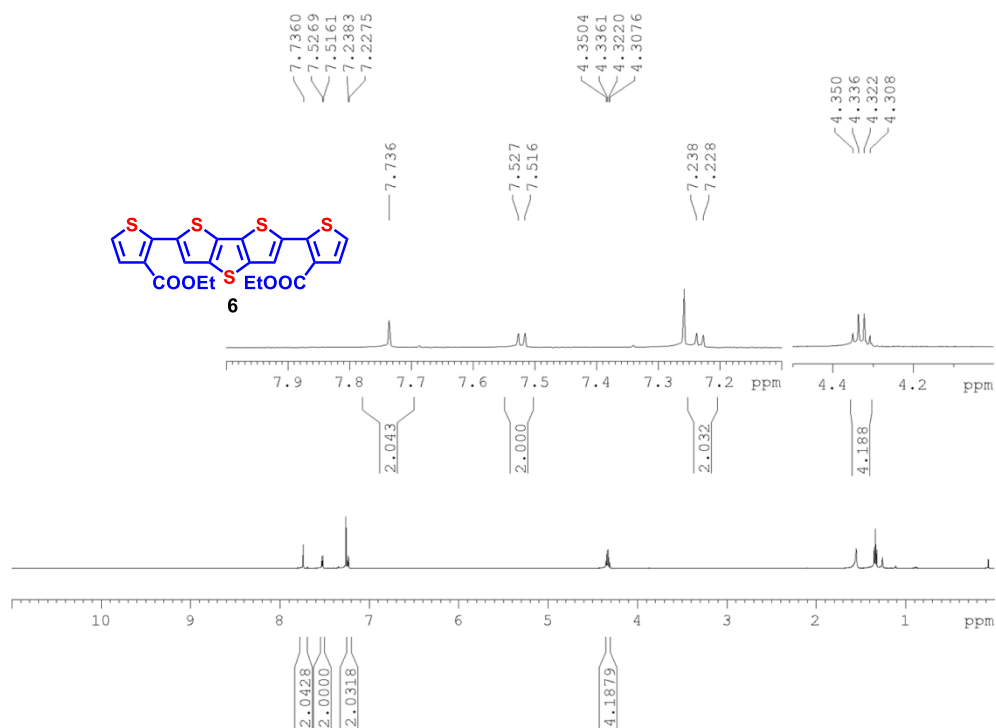
d: Thickness of the film

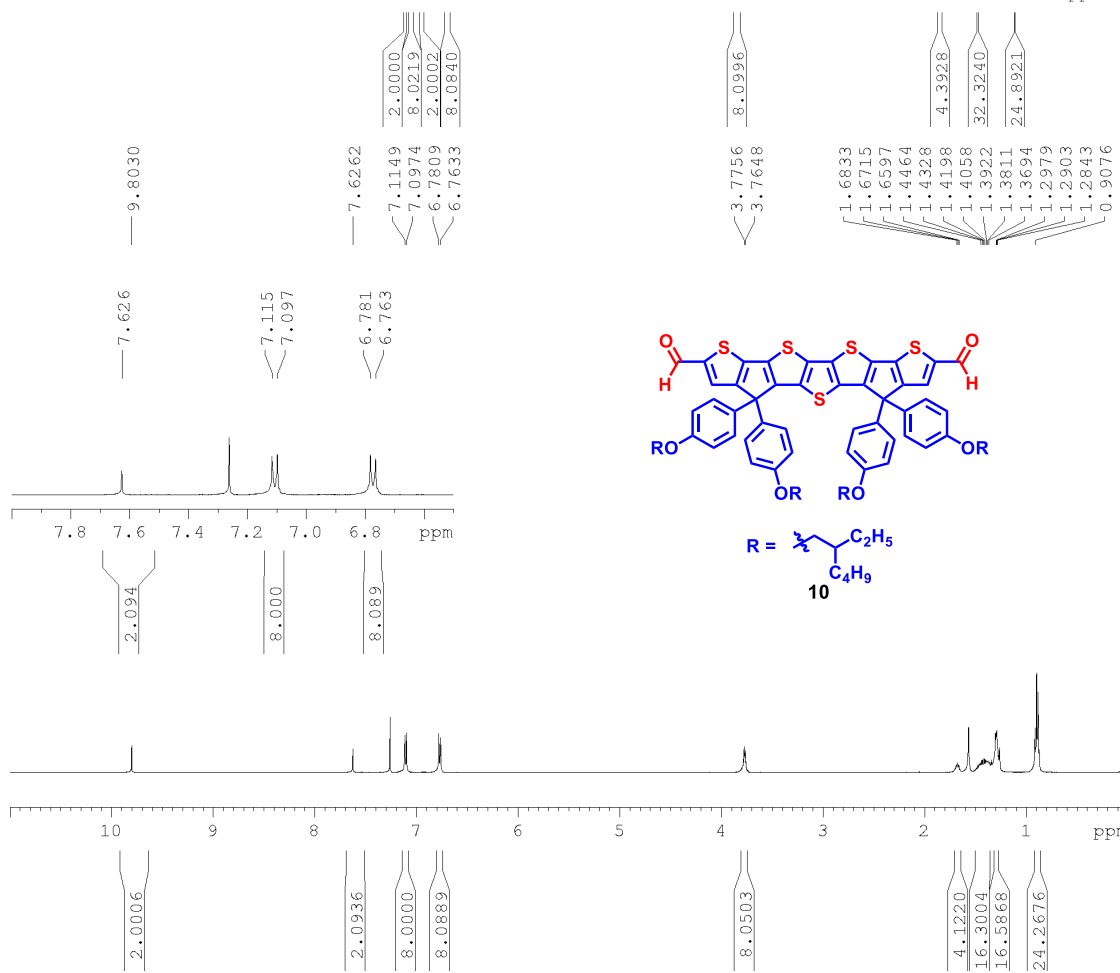
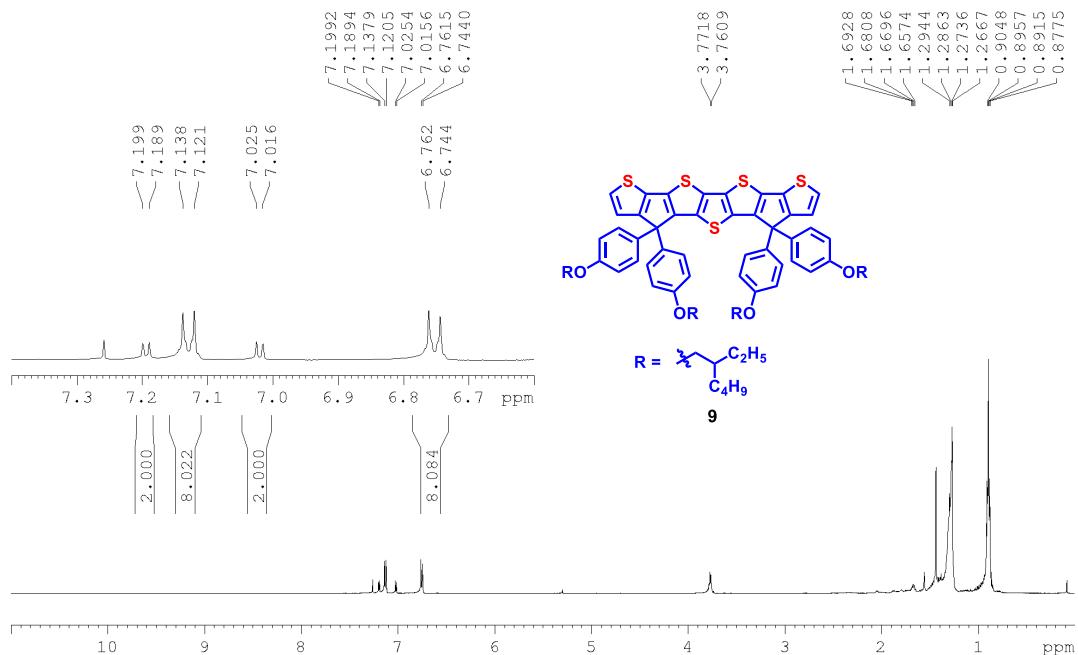
Device: FTO/c-TiO₂/m-TiO₂/Perovskite/Au

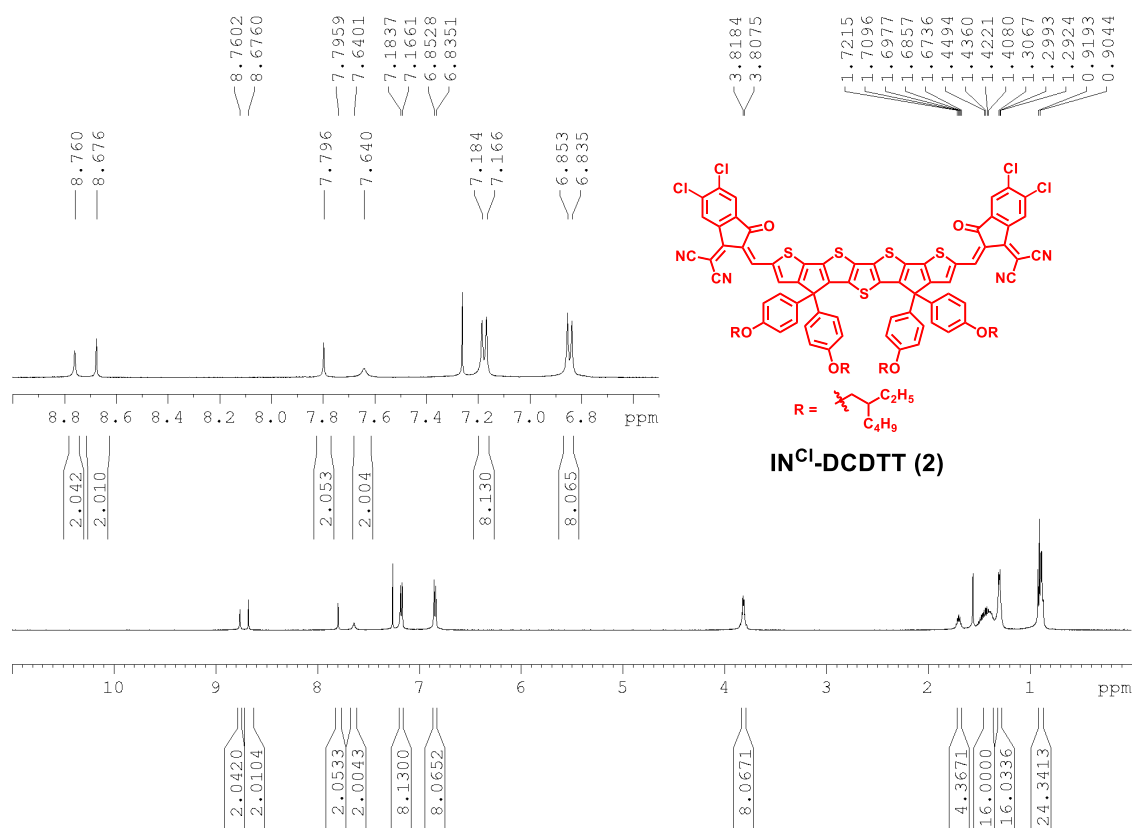
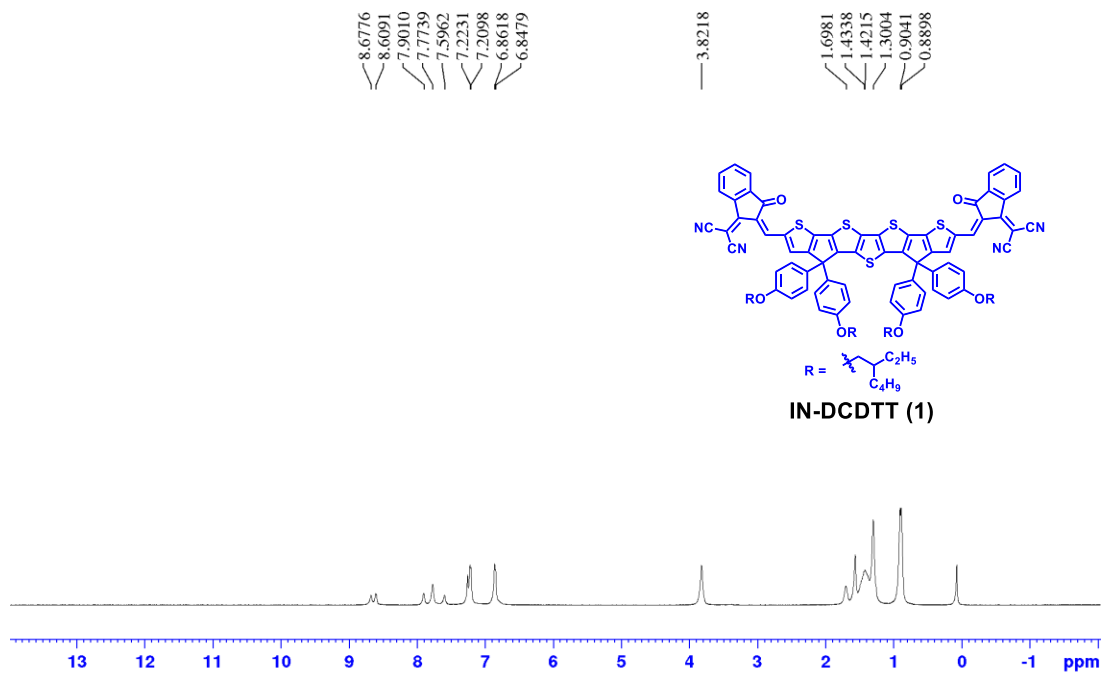
Table S7. The conductivity of the perovskite film made by using CB, 0.2 wt% **IN-DCDTT (1)_(CB)**, 0.2 wt% **IN^{Cl}-DCDTT (2)_(CB)** or 0.2 wt% **IN^{Br}-DCDTT (3)_(CB)** as an anti-solvent.

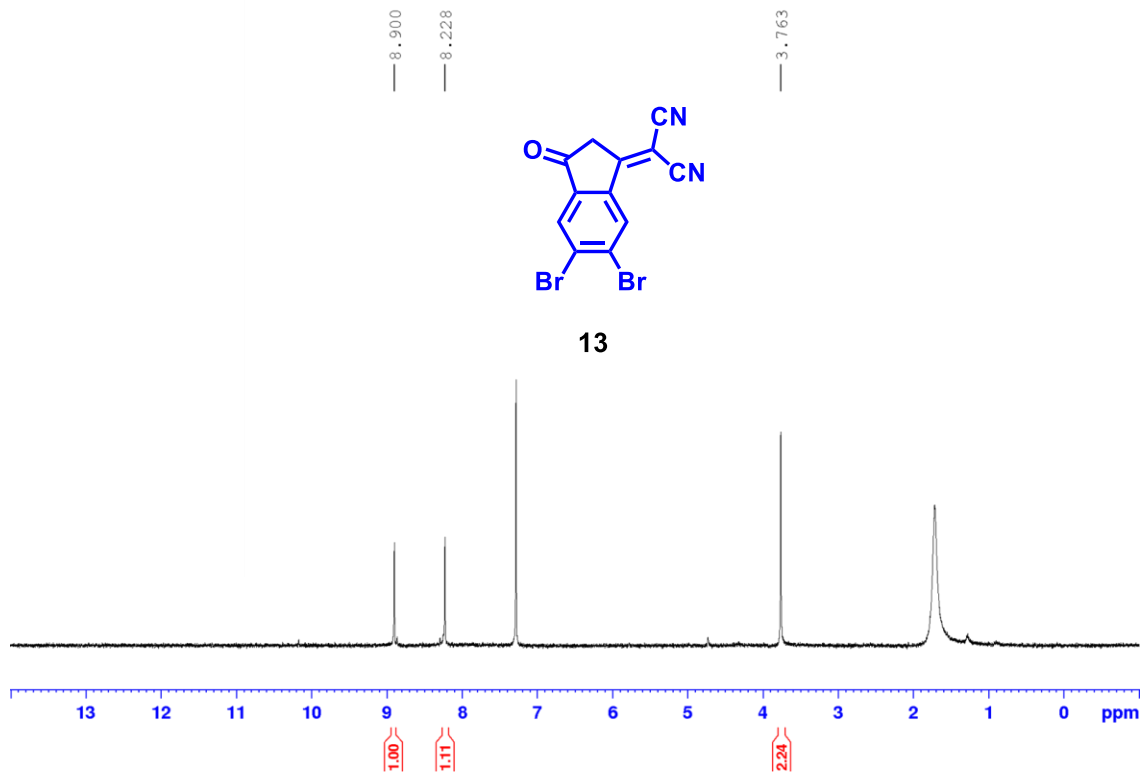
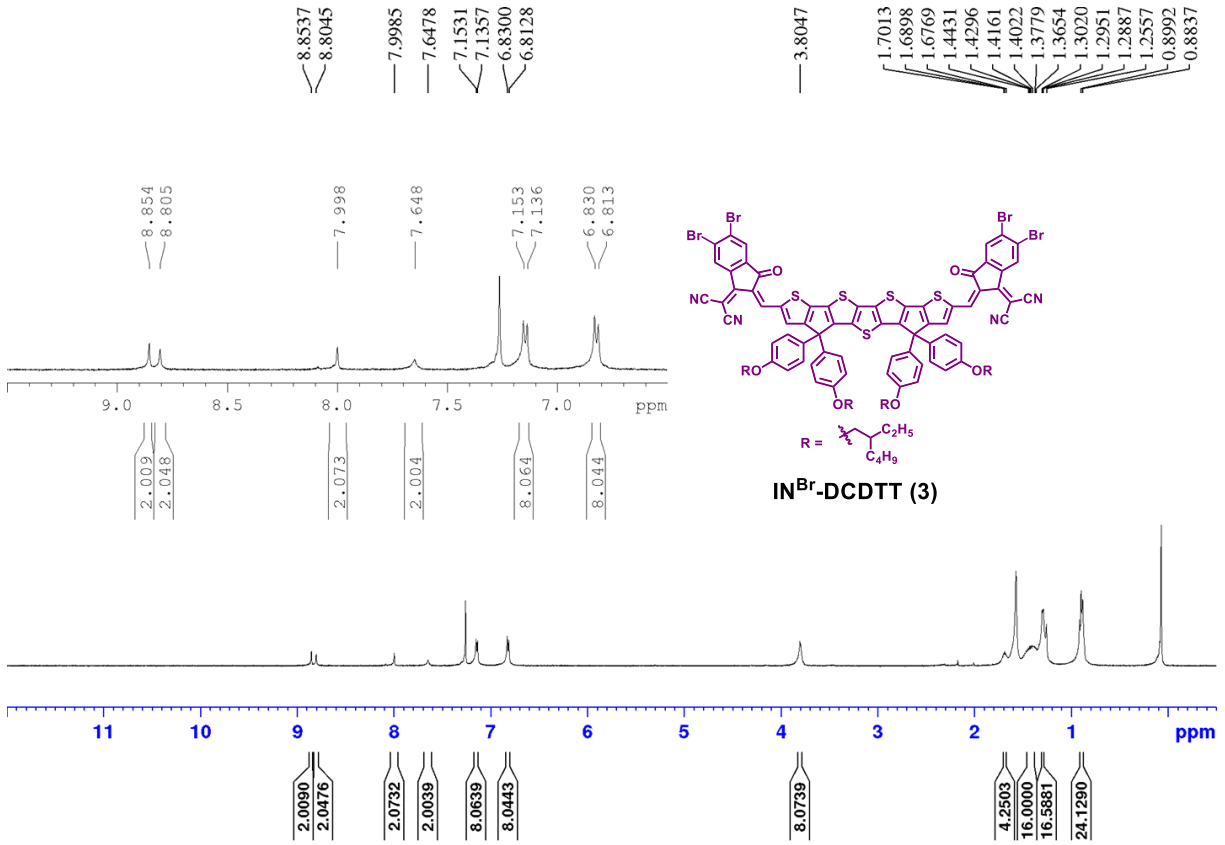
Films	Thickness of film (nm)	I/V (mA/V)	Conductivity (mS/cm)
PSK-CB	~490	27.24	1.33×10^{-2}
PSK-IN-DCDTT	~520	33.48	1.75×10^{-2}
PSK-IN ^{Cl} -DCDTT	~510	51.77	2.64×10^{-2}
PSK-IN ^{Br} -DCDTT	~490	35.93	1.75×10^{-2}

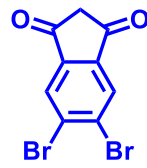
¹H NMR spectra of synthesized compounds



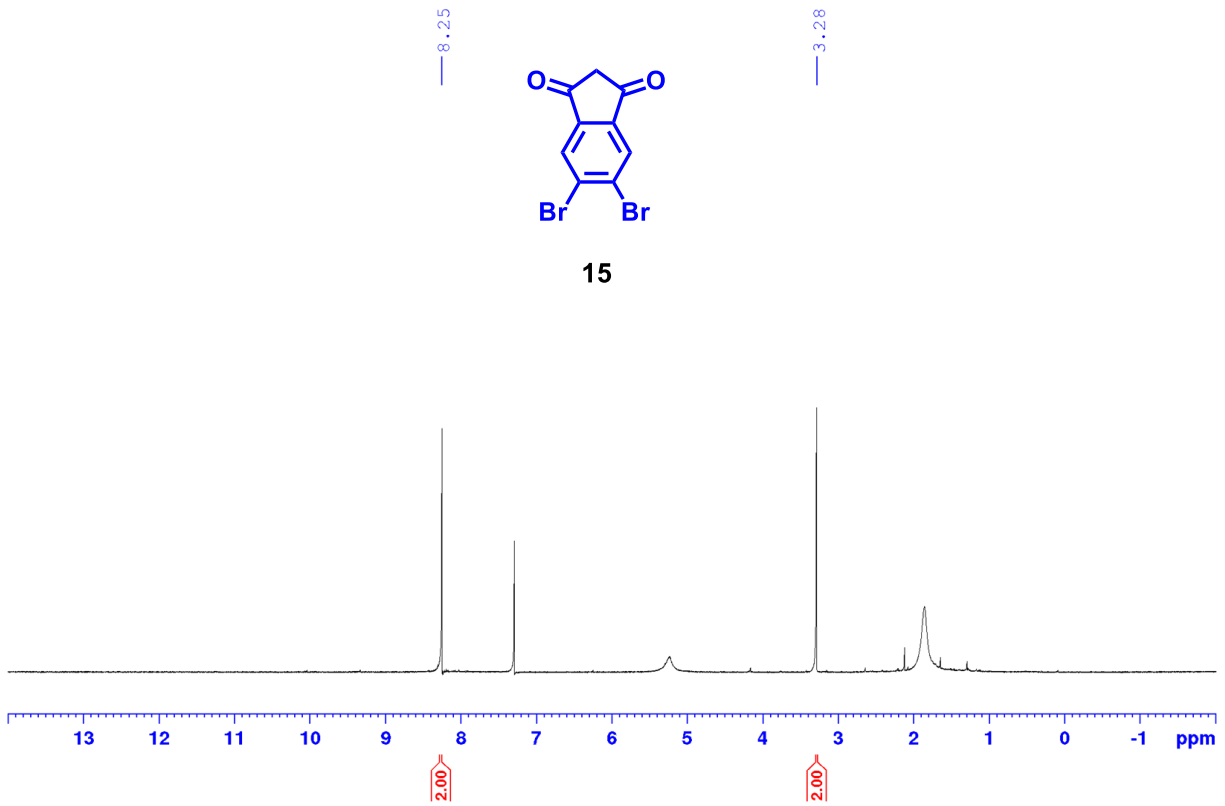




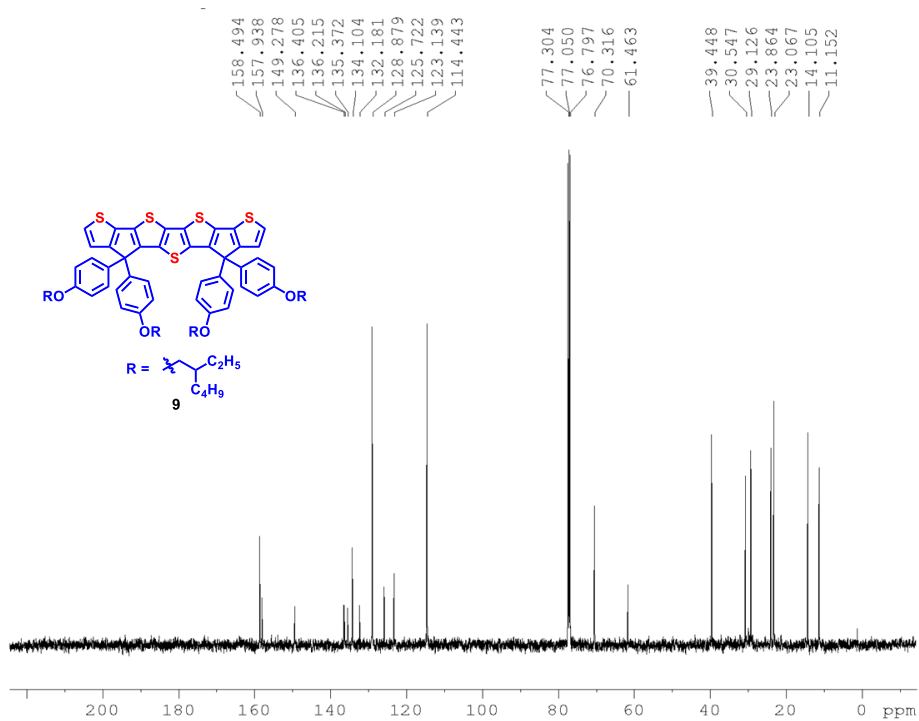
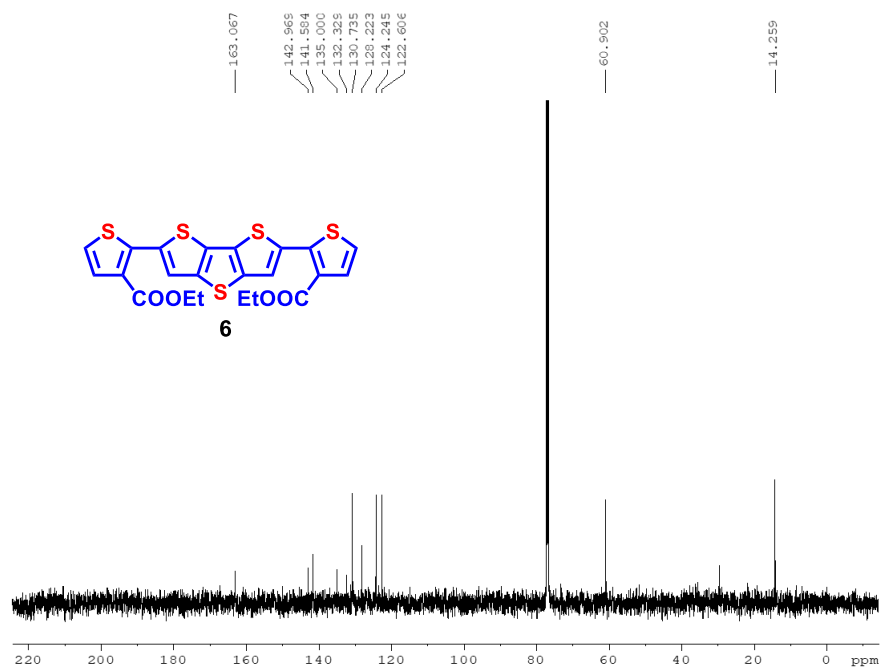


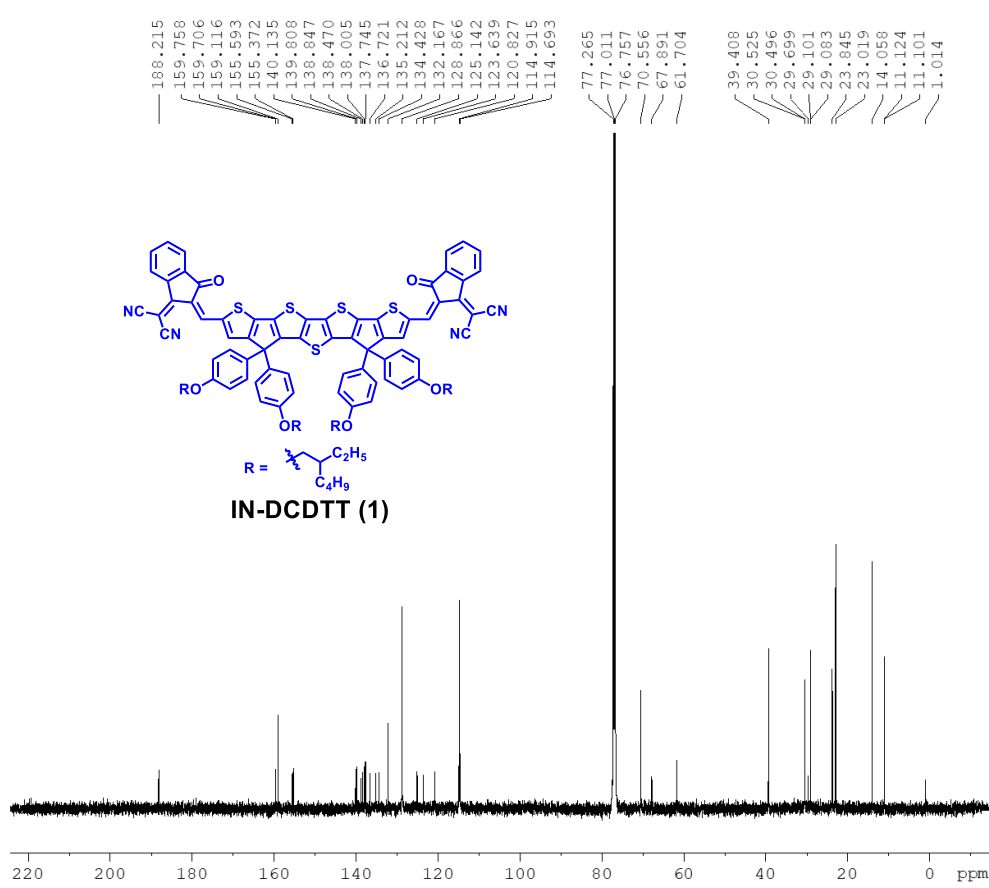
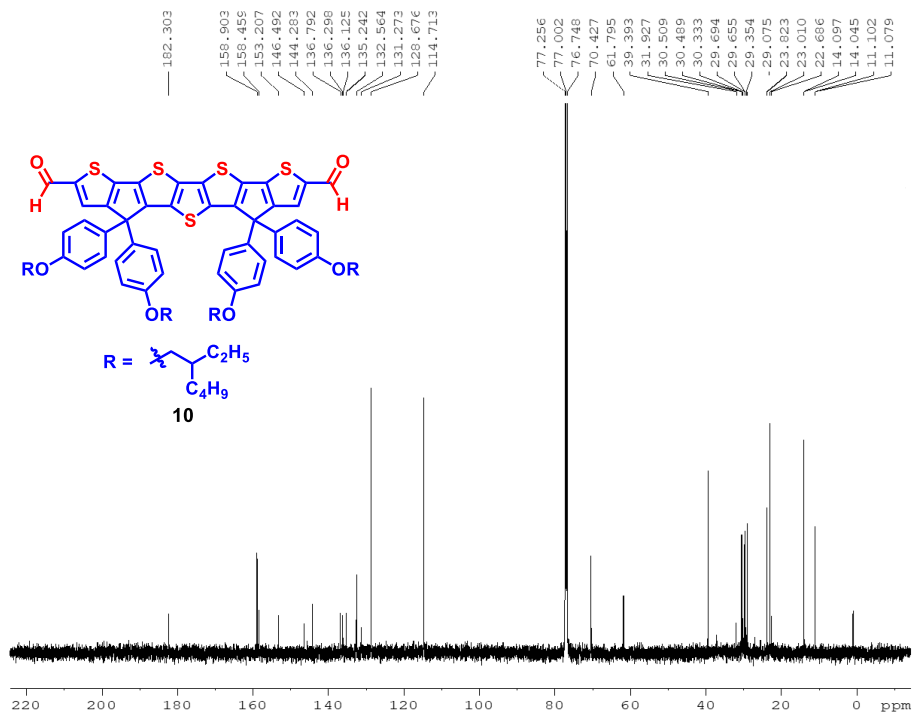


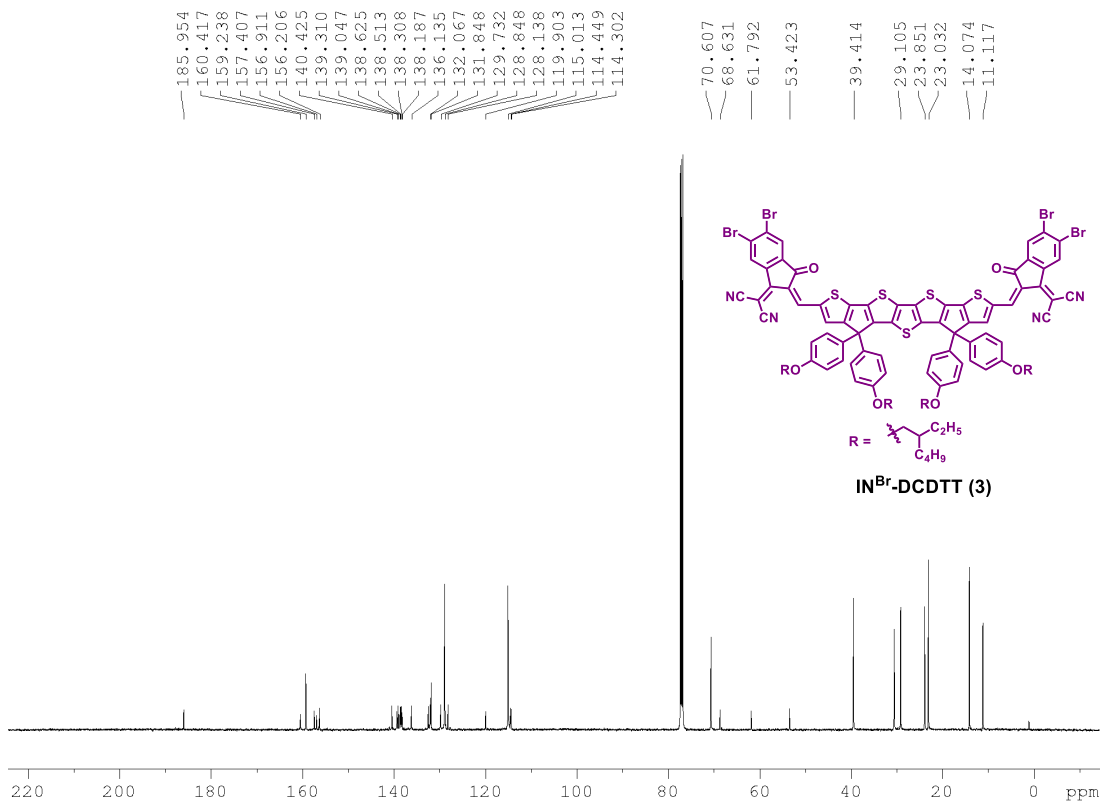
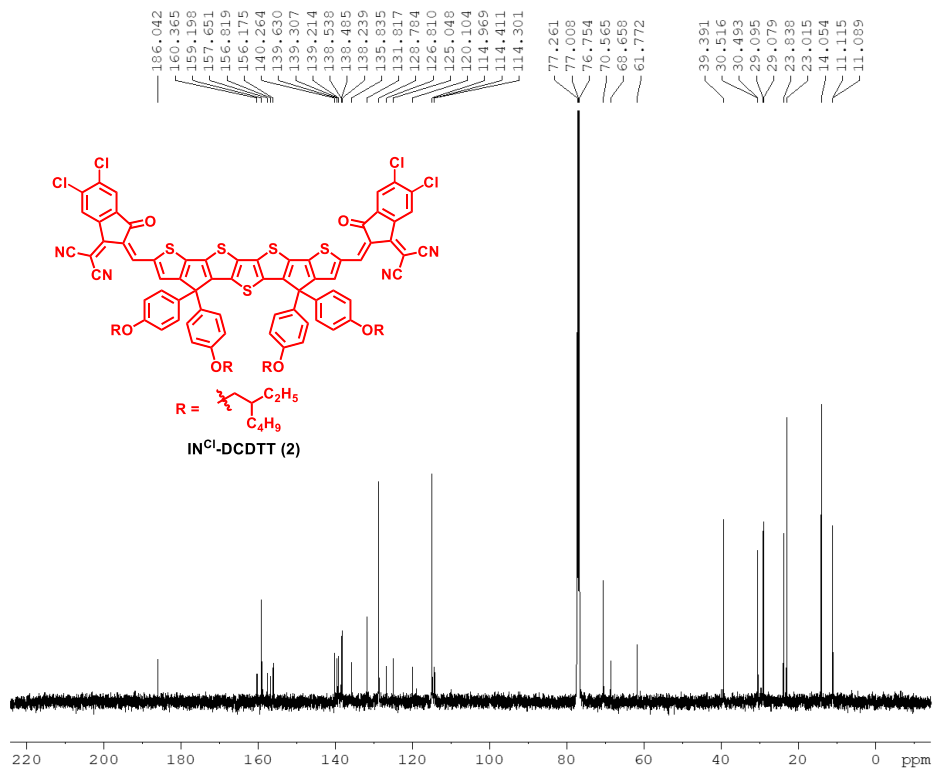
15



¹³C NMR spectra of synthesized compounds

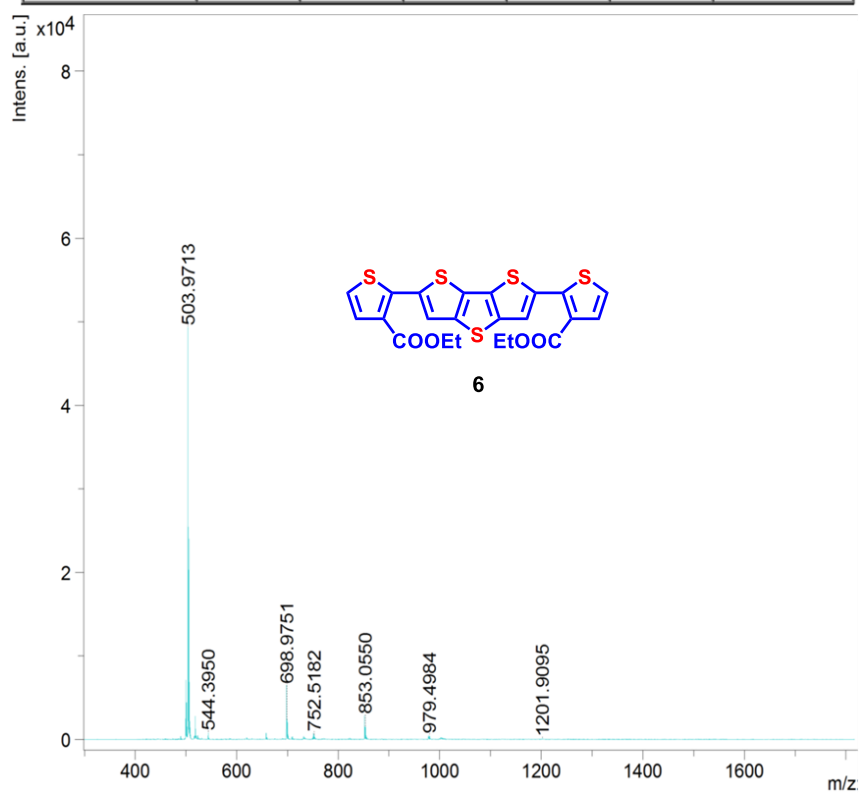




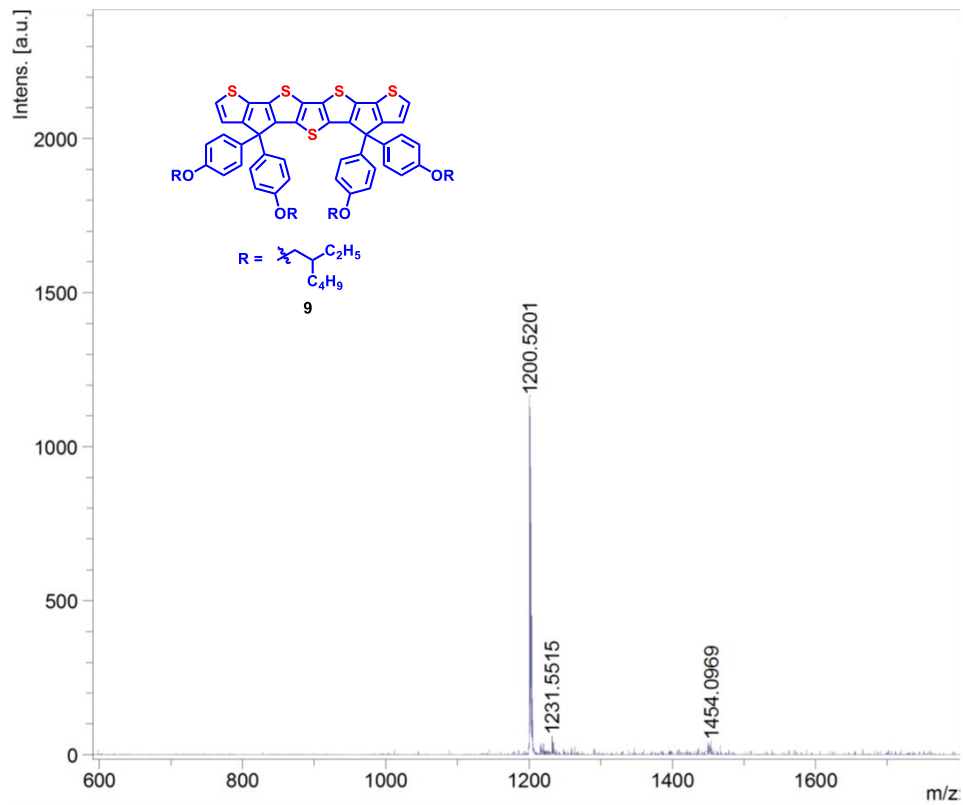


HRMS spectra of synthesized compounds

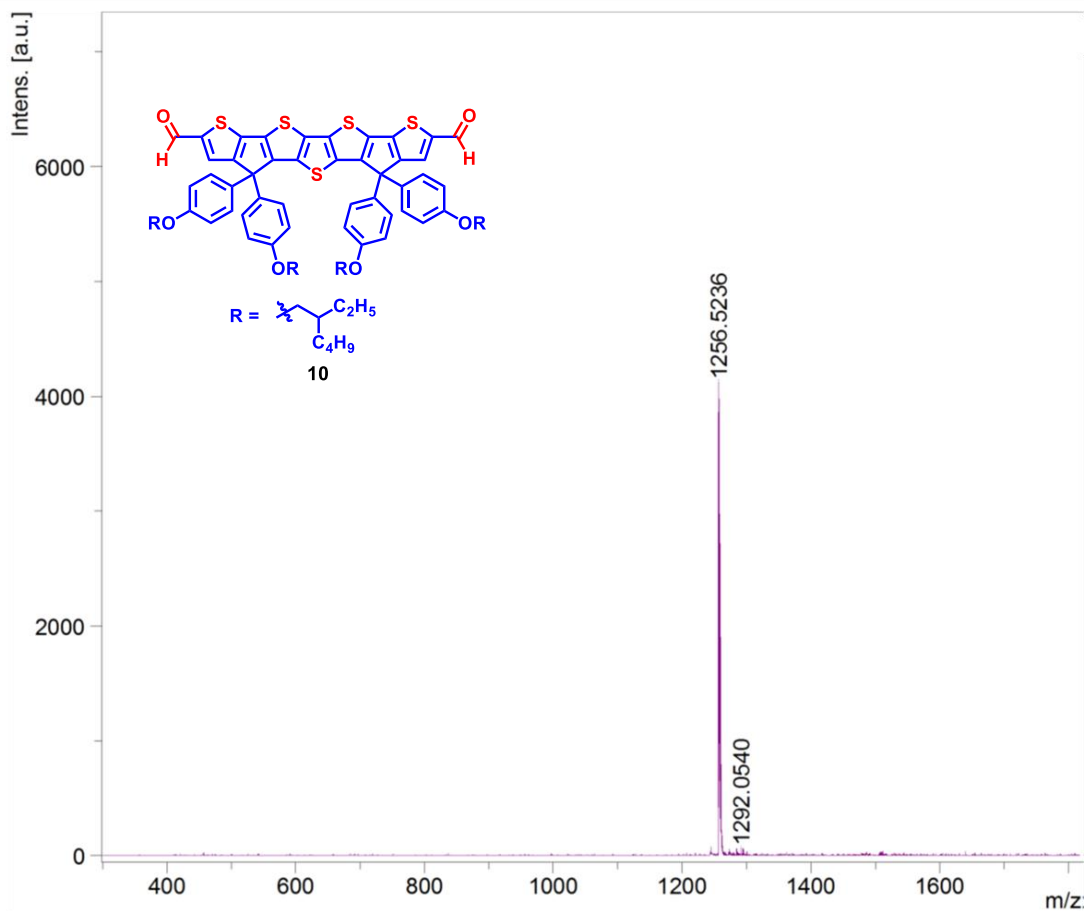
Formula	Mass	Error	mSigma	DblEq	N rule	Electron Configuration
C 22 H 16 O 4 S 5	503.9647	13.1081	800.7537	15.00	ok	odd



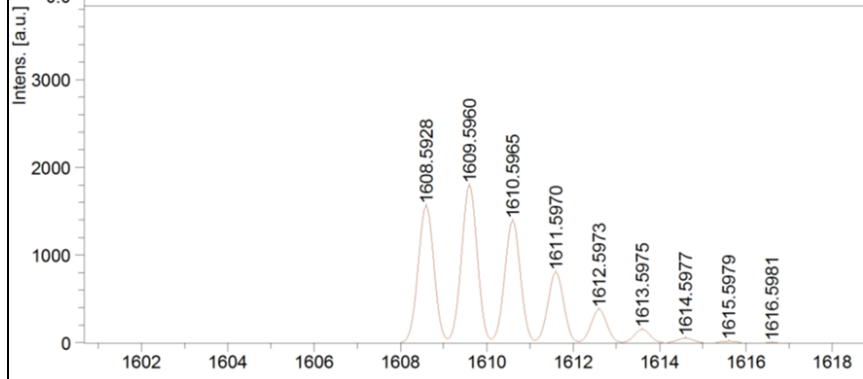
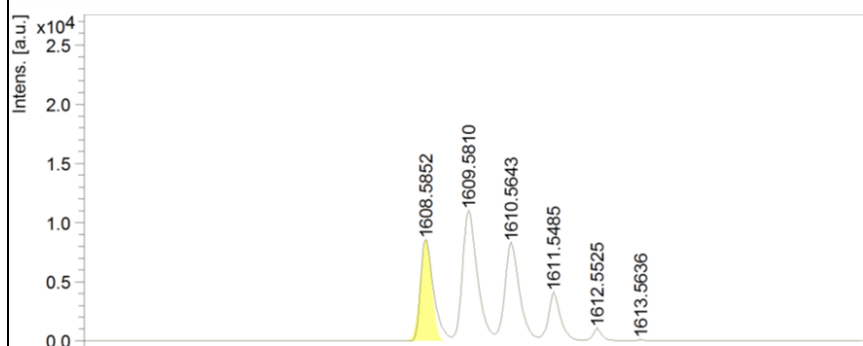
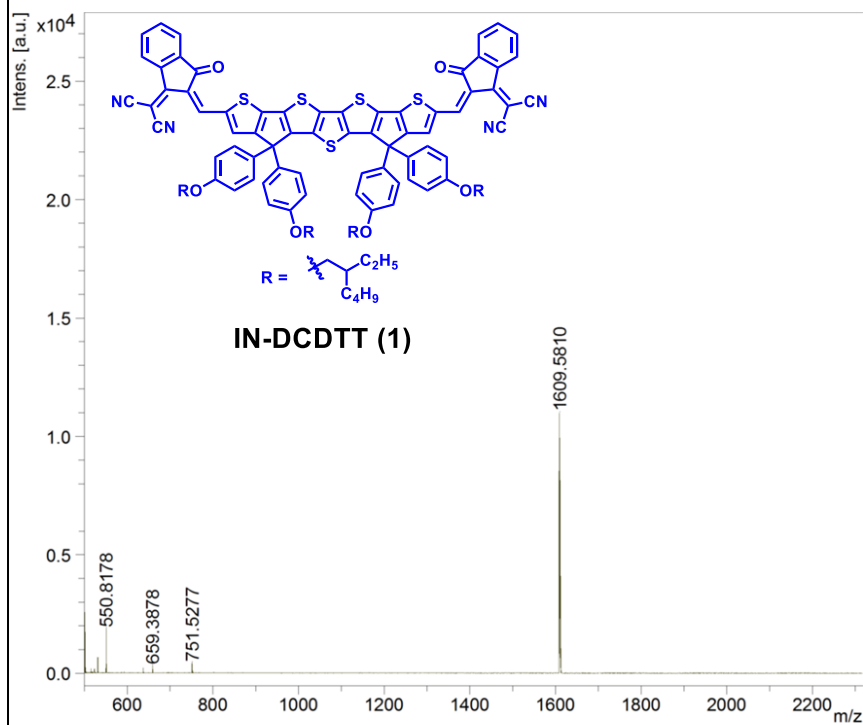
Formula	Mass	Error	mSigma	DblEq	N rule	Electron Configuration
C 74 H 88 O 4 S 5	1,200.5281	6.6369	174.3293	31.00	ok	odd



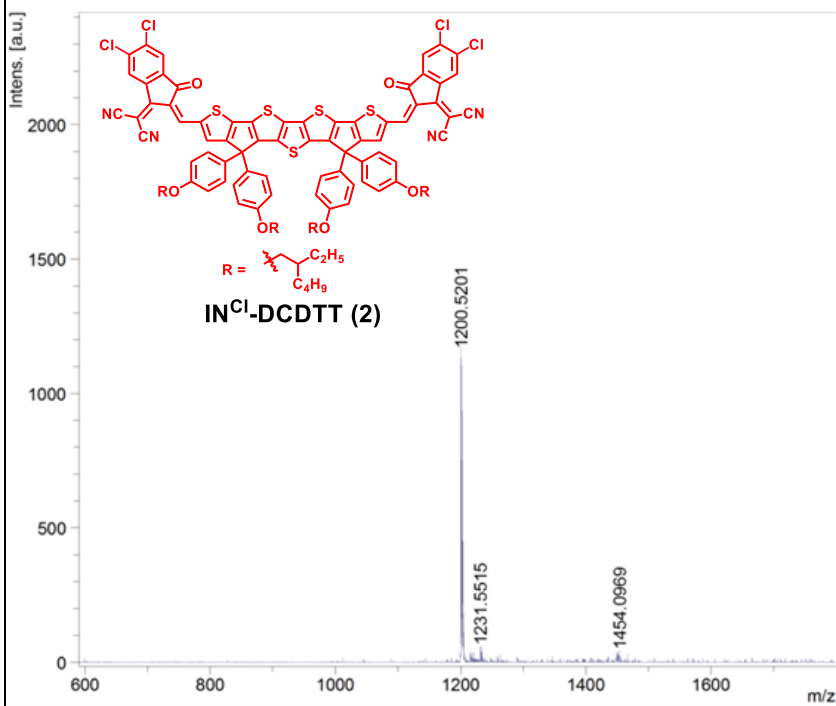
Formula	Mass	Error	mSigma	DblEq	N rule	Electron Configuration
C 76 H 88 O 6 S 5	1,256.5179	4.5387	176.1464	33.00	ok	odd



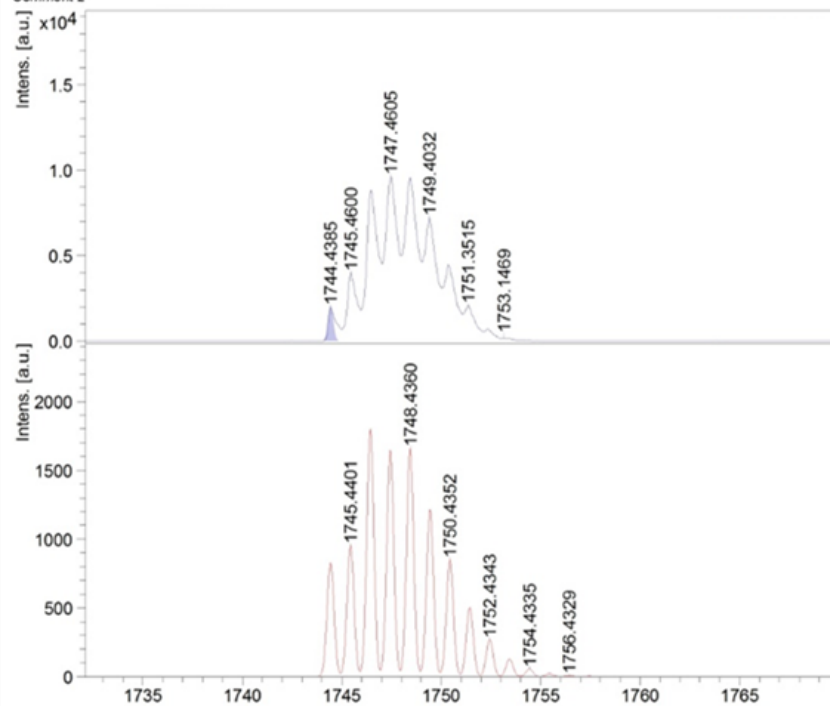
Formula	Mass	Error	mSigma	DbtEq	N rule	Electron Configuration
C ₁₀₀ H ₉₆ N ₄ O ₆ S ₅	1,608.5928	4.7485	66.5103	55.00	ok	odd



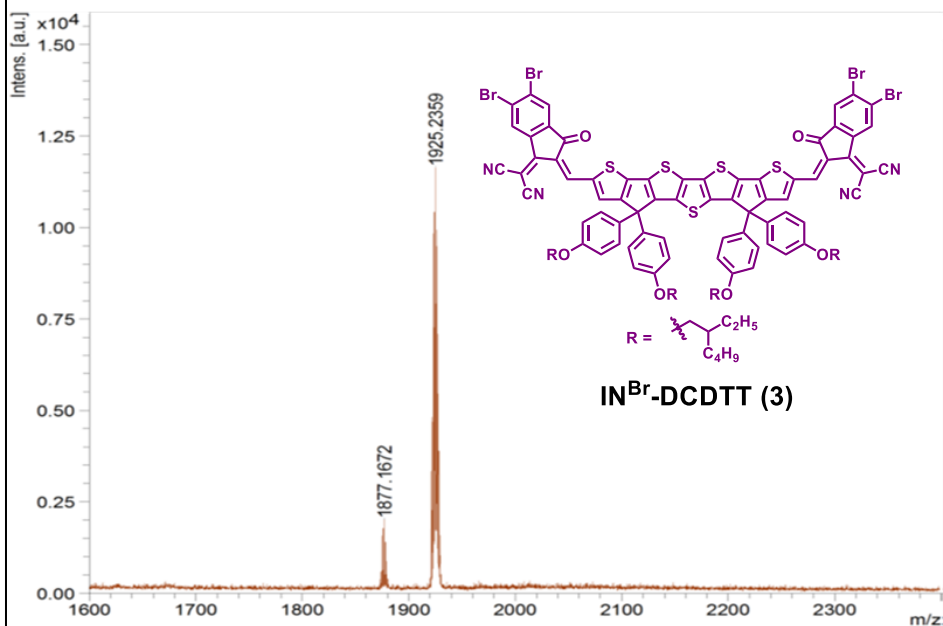
Formula	Mass	Error	mSigma	DblEq	N rule	Electron Configuration
C 100 H 92 Cl 4 N 4 O 6 S 5	1,744.4369	0.9218	94.3430	55.00	ok	odd



Comment 1
Comment 2

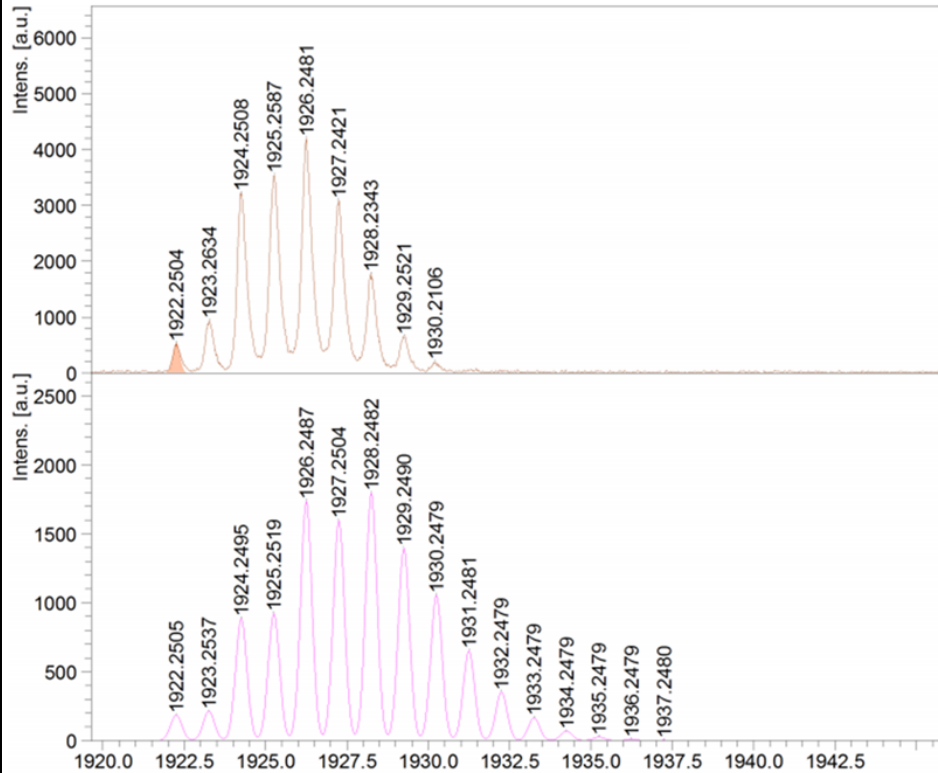


Formula	Mass	Error	mSigma	DbIEq	N rule	Electron Configuration
C 100 H 93 Br 4 N 4 O 6 S 5	1,921.2427	0.0002	270.2197	54.50	ok	even



Comment 1

Comment 2



References

1. Y. Zhang, P. Wang, M.-C. Tang, D. Barrit, W. Ke, J. Liu, T. Luo, Y. Liu, T. Niu, D.-M. Smilgies, Z. Yang, Z. Liu, S. Jin, M. G. Kanatzidis, A. Amassian, S. F. Liu and K. Zhao, *J. Am. Chem. Soc.*, 2019, **141**, 2684-2694.
2. F. N. Mott and R. W. Gurney, *Electronic Process in Ionic Crystals*, 1940, 1st ed, Oxford University Press.
3. A. G. Baradwaj, L. Rostro, M. A. Alam and B. W. Boudouris, *Appl. Phys. Lett.*, 2014, **104**, 213306.